

Anomalous spatio-temporal chaos in a two-dimensional system of non-locally coupled oscillators

Hiroya Nakao*

Department of Physics, Graduate School for Sciences, Kyoto University, Kyoto 606-8502, Japan

(March 8, 1999)

A two-dimensional system of non-locally coupled complex Ginzburg-Landau oscillators is investigated numerically for the first time. As already known for the one-dimensional case, the system exhibits anomalous spatio-temporal chaos characterized by power-law spatial correlations. In this chaotic regime, the amplitude difference between neighboring elements shows temporal noisy on-off intermittency. The system is also spatially intermittent in this regime, which is revealed by multi-scaling analysis; the amplitude field is multi-affine and the difference field is multi-fractal. Correspondingly, the probability distribution function of the measure defined for each field is strongly non-Gaussian, showing scale-dependent deviations in the tails due to intermittency.

Assemblies of mutually interacting dynamical units are ubiquitous in nature. As models for them, systems of coupled simple dynamical elements, e.g. limit cycle oscillators or chaotic maps, have been studied extensively. Recently, a new class of coupled systems, namely, a system with non-locally coupled dynamical elements, was introduced and found to exhibit anomalous spatio-temporal chaos characterized by power-law spatial correlations. The preceding studies on this system have been done in one dimension, but the mechanism for the appearance of this spatio-temporal chaos seems to be universal, and it is also expected in higher dimensions. In this paper, a two-dimensional system of non-locally coupled oscillators is investigated for the first time. As in the one-dimensional case, the system is found to exhibit anomalous spatio-temporal chaos, accompanied by several distinctive features specific to this chaotic regime, i.e., power-law spatial correlations, noisy on-off intermittency, and multi-scaling properties.

I. INTRODUCTION

Assemblies of dynamical elements coupled with each other are widely seen in nature. Simplified models of such systems, e.g. coupled limit cycle oscillators or chaotic maps, have played important roles not only in modeling such systems realistically, but also in understanding the varieties of possible behavior of systems far from equilib-

rium. Many important concepts, such as pattern formation or spatio-temporal chaos, have been extracted from the detailed studies on such models.

The interaction between the elements are usually assumed to be attractive, and of mean-field type in a wide sense; each element feels the mean amplitude of its neighboring elements, and driven by the difference between its amplitude and the mean amplitude, in such a way that the amplitude differences between the elements decrease.

The diffusive coupling is a representative limiting case. Each element interacts strongly with its nearest neighbors, so that the amplitude field of the system is always continuous and smooth. It is well known that some diffusively coupled systems of dynamical elements, such as the complex Ginzburg-Landau equation, exhibit spatio-temporal chaos [1,2].

The opposite limiting case is the global coupling, or the mean field coupling in the narrow sense. Each element feels the mean field of the entire system, and is thus coupled to all the elements with equal strength. The amplitude field becomes statistically spatially homogeneous, and the notion of space is lost. It is known that systems with global coupling generally show some typical behavior, e.g. clustering and collective chaos [3,4].

In Ref. [5], Kuramoto introduced an intermediate system between the above two limiting cases, namely a system of non-locally coupled elements. Our subsequent numerical simulations of one-dimensional non-locally coupled systems with various elements revealed that such systems generally exhibit anomalous spatio-temporal chaotic behavior, which cannot be seen in the above two limiting cases. In this chaotic regime, the amplitude field becomes fractal, and the spatial correlation of the amplitude field shows power-law behavior on small scales. Furthermore, the fractal dimension and the exponent of the spatial correlation vary continuously with the coupling strength. Later, we developed a theory that can explain the fractality of the amplitude field and the power-law behavior of the spatial correlation based on a simple multiplicative stochastic model [6,7]. Such a model is frequently employed in describing the noisy on-off intermittency phenomena [8–10] found in many physical systems, and this implies that our system should also exhibit this type of temporal intermittency. Induced by the temporal intermittency, our system is also spatially intermittent. In order to study this, we expanded our analysis of the amplitude field into more general q -th structure functions, and found that the amplitude field shows multi-affinity. We also introduced multi-fractal

analysis of the difference field of the original amplitude field, inspired by its seeming similarity to the intermittent energy dissipation field in fluid turbulence [6,11].

All our previous studies have been done in one-dimensional systems. However, our previous theory does not require the systems to be one-dimensional, and spatio-temporal chaos with power-law structure functions is also expected in higher dimensions. In this paper, we study a system of non-locally coupled complex Ginzburg-Landau oscillators in two dimensions for the first time, and investigate its anomalous spatio-temporal chaotic regime. Some attention is paid to the multi-scaling properties of the intermittent amplitude and difference fields.

II. MODEL

As proposed by Kuramoto [5], the non-local coupling naturally appears in the following plausible situation. Consider an assembly of spatially distributed dynamical elements, e.g. cells. Each element is assumed to interact indirectly with other elements through some (e.g. chemical) substance, which diffuses and decays much faster than the dynamics of the element. Such a situation will be described by the following set of equations:

$$\dot{\mathbf{X}}(\mathbf{r}, t) = \mathbf{F}(\mathbf{X}(\mathbf{r}, t)) + \mathbf{K} \cdot \mathbf{A}(\mathbf{r}, t), \quad (1)$$

$$\epsilon \dot{\mathbf{A}}(\mathbf{r}, t) = -\eta \mathbf{A}(\mathbf{r}, t) + D \nabla^2 \mathbf{A}(\mathbf{r}, t) + \mathbf{X}(\mathbf{r}, t), \quad (2)$$

where \mathbf{X} is the amplitude of the element, \mathbf{F} is the dynamics of the amplitude, and \mathbf{A} is the concentration of the substance with decay rate η and diffusion rate D . The substance \mathbf{A} is generated at a rate proportional to the amplitude \mathbf{X} , and the amplitude \mathbf{X} is affected by the substance \mathbf{A} with a coupling matrix \mathbf{K} . The parameter ϵ determines the ratio of time scale of the elements to that of the substance, and is assumed to be very small. Namely, the dynamics of the substance is much faster than that of the elements.

Now, let us consider the $\epsilon \rightarrow 0$ limit and eliminate the dynamics of \mathbf{A} adiabatically. Putting the left-hand side of Eq.(2) to 0, we can solve the equation for \mathbf{A} as

$$\mathbf{A}(\mathbf{r}, t) = \int d\mathbf{r}' G(\mathbf{r}' - \mathbf{r}) \mathbf{X}(\mathbf{r}', t), \quad (3)$$

where $G(\mathbf{r}' - \mathbf{r})$ is a kernel that satisfies

$$(\eta - D \nabla^2) G(\mathbf{r}' - \mathbf{r}) = \delta(\mathbf{r}'). \quad (4)$$

By inserting Eq.(3) into Eq.(1), we obtain the following system of non-locally coupled dynamical elements:

$$\dot{\mathbf{X}}(\mathbf{r}, t) = \mathbf{F}(\mathbf{X}(\mathbf{r}, t)) + \mathbf{K} \cdot \int d\mathbf{r}' G(\mathbf{r}' - \mathbf{r}) \mathbf{X}(\mathbf{r}', t). \quad (5)$$

The kernel $G(\mathbf{r}' - \mathbf{r})$ can be solved as

$$G(\mathbf{r}' - \mathbf{r}) = \frac{1}{(2\pi)^d} \int d^d \mathbf{q} \frac{\exp[i\mathbf{q} \cdot (\mathbf{r}' - \mathbf{r})]}{\eta + D|\mathbf{q}|^2}, \quad (6)$$

where d is the dimension of the space. When the system is isotropic, the kernel G becomes a function of the distance $r := |\mathbf{r}' - \mathbf{r}|$, and is expressed as

$$G(r) \propto \exp(-\gamma|r|) \quad d=1, \quad (7)$$

$$K_0(\gamma|r|) \quad d=2, \quad (8)$$

$$\frac{\exp(-\gamma|r|)}{\gamma|r|} \quad d=3, \quad (9)$$

where K_0 is the modified Bessel function. The constant γ gives the inverse of the coupling length, and is calculated as

$$\gamma = \sqrt{\frac{\eta}{D}}. \quad (10)$$

Each $G(r)$ must satisfy the normalization condition $\int G(r) d^d \mathbf{r} = 1$. Since we treat a two-dimensional system, we use Eq.(8) for $G(r)$ hereafter.

As elements, we use complex Ginzburg-Landau oscillators. They are the simplest limit cycle oscillators that can be derived by the center-manifold reduction technique from generic oscillators near their Hopf bifurcation points [1]. The corresponding non-locally coupled system is given by the following equation for the complex amplitude W :

$$\dot{W}(\mathbf{r}, t) = W - (1 + ic_2)|W|^2 W + K(1 + ic_1)(\bar{W} - W), \quad (11)$$

where K is the coupling strength, c_1, c_2 are real parameters, and the non-local mean field \bar{W} is given by

$$\bar{W}(\mathbf{r}, t) = \int d\mathbf{r}' G(\mathbf{r}' - \mathbf{r}) W(\mathbf{r}', t). \quad (12)$$

This is the non-local complex Ginzburg-Landau equation introduced by Kuramoto [5] as the first concrete example of non-locally coupled systems.

III. ANOMALOUS SPATIO-TEMPORAL CHAOS

In the numerical simulations presented here, we assume the total system to be a square lattice with both sides unit length long. The elements are placed on the lattice sites, and periodic boundary conditions are assumed. We use $N^2 = 512^2 \sim 1024^2$ elements, and fix the coupling length γ^{-1} at 1/8. The non-local mean field is easily calculated by using the FFT technique, since it is simply a convolution of the amplitude field with the kernel (8). We fix the parameters c_1 and c_2 at -2 and 2 respectively. These are the standard values already used in our previous one-dimensional simulations.

In Fig.1-3, typical snapshots of the real part $X(x, y)$ of the complex variable $W(x, y)$ are shown for three different values of coupling strength K . Since we obtain similar figures for the imaginary part $Y(x, y)$ by symmetry, we use $X(x, y)$ in the following analysis and call it amplitude field. The amplitude field at $K = 1.05$ is continuous and smooth, while at $K = 0.65$ it seems to be discontinuous and disordered, although not completely random. The amplitude field at the intermediate coupling strength $K = 0.85$ looks somewhat more complex and intriguing; it is composed of intricately convoluted smooth and disordered patches of various length scales. This is the anomalous spatio-temporal chaotic regime that our interest is focused on.

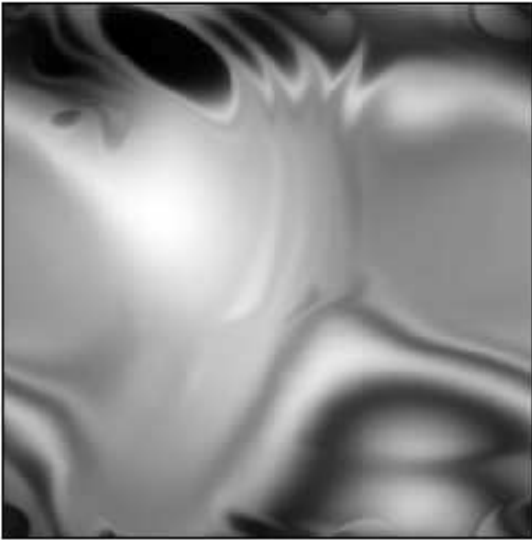


FIG. 1. Snapshot of the amplitude field $X(x, y)$ at $K = 1.05$. Darker dots indicates larger amplitudes.

IV. SPATIAL CORRELATION FUNCTION

Let us examine the spatial correlation function first. Figures 4(a)-(c) show spatial correlation functions $C(x, y) := \langle X(0, 0)X(x, y) \rangle$ corresponding to the amplitude fields shown in Figs.1-3. Each correlation function is clearly rotationally symmetric due to the isotropy of the system. As the amplitude field becomes disordered, the correlation function becomes steep, and the center of the graph, which corresponds to the self-correlation $C(0, 0)$, becomes peaked.

In Ref. [5], the anomalous spatio-temporal chaotic regime was characterized by the power-law behavior of the spatial correlation function in small distance:

$$C(l) := \langle X(0)X(l) \rangle \simeq C_0 - C_1 l^\alpha \quad (l \ll 1), \quad (13)$$

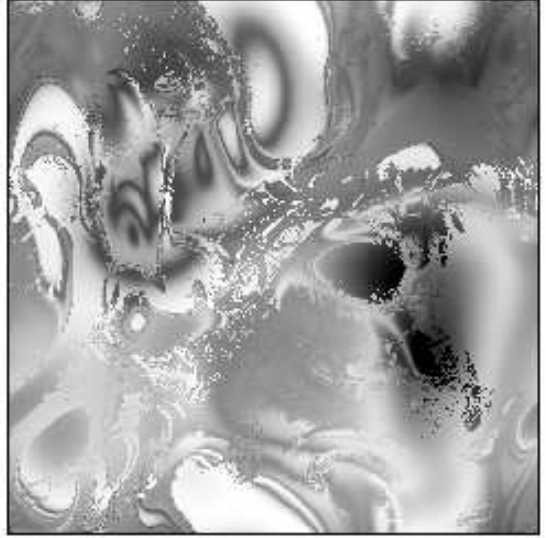


FIG. 2. Snapshot of the amplitude field $X(x, y)$ at $K = 0.85$.

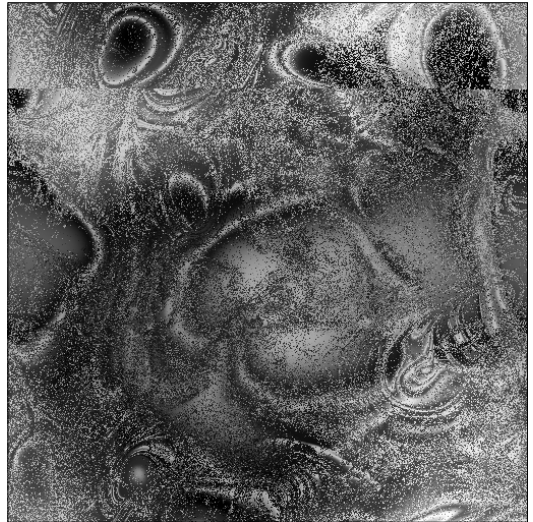


FIG. 3. Snapshot of the amplitude field $X(x, y)$ at $K = 0.65$.

where C_0, C_1 are constants and α is a non-integer parameter-dependent exponent.

To confirm if this power-law behavior also holds in two dimension, we calculated the radial correlation function $C(l) = \langle X(\mathbf{r})X(\mathbf{r}+\mathbf{l}) \rangle$ ($|\mathbf{l}| = l$) along a straight line in a certain direction¹, and estimated the best fitting parameters C_0 and C_1 . Figure 5 shows $\ln l$ vs. $\ln [C_0 - C(l)]$ for several values of the coupling strength K . For each coupling strength, the experimental data are almost on a straight line, and the power-law behavior is evident. The exponent α of the power law varies continuously with the coupling strength. Although not shown in the figure, the correlation function $C(l)$ is continuous at the origin $l = 0$ for $K \geq 0.85$, but discontinuous at $K = 0.80$. There appears a finite gap between the self-correlation $C(0)$ and the correlation between the nearest-neighbor elements $\lim_{l \rightarrow +0} C(l) \simeq C_0$. This means that the individual motion of the element becomes so violent that the amplitude field is no longer continuous statistically. In Ref. [7], this transition point was identified with the blowout bifurcation point in the on-off intermittent dynamics of the amplitude difference between nearby elements.

Thus, the anomalous spatio-temporal chaos in two dimension is also characterized by power-law behavior of the spatial correlation function with a parameter-dependent exponent.

V. NOISY ON-OFF INTERMITTENCY

In Ref. [6,7], we clarified that the scaling behavior of the spatial correlation is a consequence of underlying multiplicative processes of amplitude differences between neighboring elements. We described this process by a multiplicative stochastic model, and related the exponent α of the spatial correlation with the fluctuation of the finite-time Lyapunov exponent of the element. Such a model is essentially identical with those used in describing noisy on-off intermittency [8–10], which indicates that our system also exhibits this type of temporal intermittency. Actually, the finite-time Lyapunov exponent of the complex Ginzburg-Landau oscillator can fluctuate between positive and negative values, and neighboring oscillators are subjected to only slightly different non-local mean field. Therefore, the conditions for the appearance of noisy on-off intermittency are satisfied in our system.

Now, let us confirm this in our system numerically. The coupling strength is set at $K = 0.85$. Figure 6 shows typical time sequences of amplitude differences $\Delta X_1(t)$ and $\Delta X_2(t)$. The distance between the elements is 512^{-1} for $\Delta X_1(t)$, and 64^{-1} for $\Delta X_2(t)$, respectively. Strong

¹We mainly used the (0, 1) or the (1, 1) direction, but results are independent of the direction.

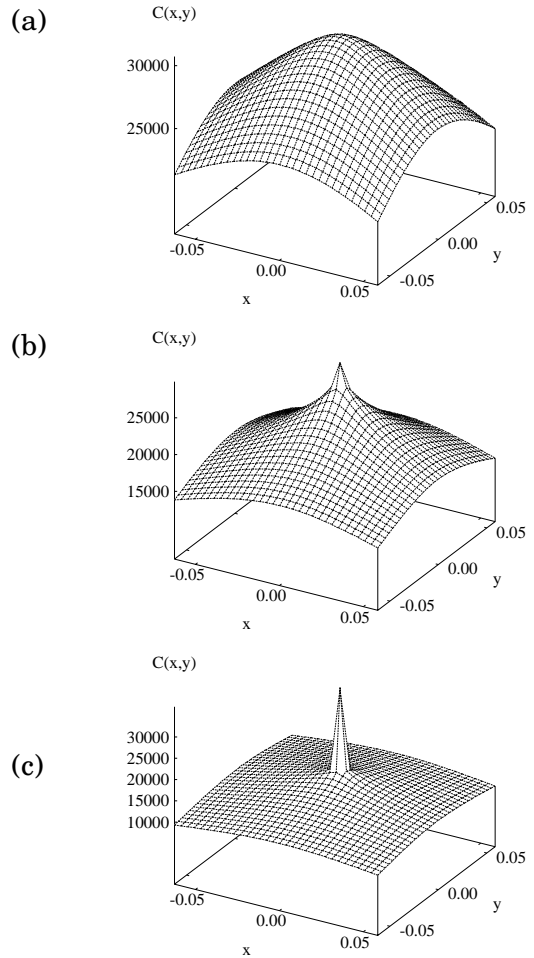


FIG. 4. Short-range spatial correlation functions $C(x, y)$ at (a) $K = 1.05$, (b) $K = 0.85$, and (c) $K = 0.65$.

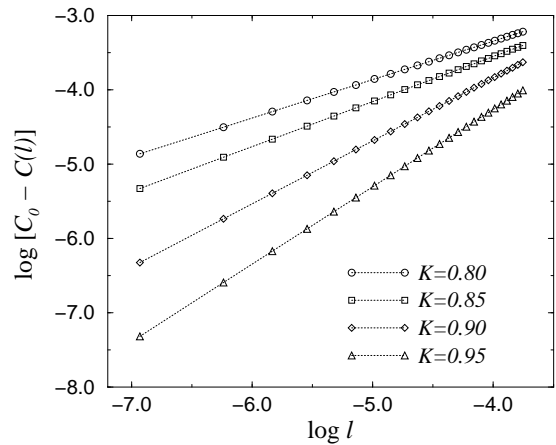


FIG. 5. Power-law behavior of the correlation functions; log-log plot of $C_0 - C(l)$ vs. l obtained for several values of the coupling strength K .

intermittency of the signals is apparent. It can be seen that $\Delta X_2(t)$ shows more frequent bursts than $\Delta X_1(t)$, reflecting that $\Delta X_2(t)$ is subjected to larger fluctuations than $\Delta X_1(t)$.

We can confirm that these intermittent signals are actually noisy on-off intermittent by calculating the laminar length distribution. The laminar phase is defined as a successive duration where the absolute value of the difference does not exceeds a certain threshold. Here we choose 0.5 as the threshold value. Figure 7 shows laminar length distributions $R(t)$ obtained from $\Delta X_1(t)$ and $\Delta X_2(t)$. The characteristic shape of the distribution $R(t)$, i.e., the power-law dependence on t with slope $-3/2$ for small t , and the exponential shoulder seen in the large t region, clearly indicates that the signals are actually noisy on-off intermittent. The shoulder reflects broken scale invariance due to the additive noise. As expected, the shoulder of $\Delta X_2(t)$ appears at a smaller value of t than that of $\Delta X_1(t)$ [9,10].

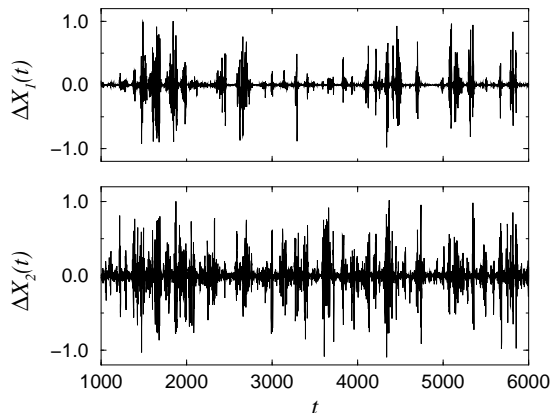


FIG. 6. Typical temporal evolution of the amplitude differences. The distance between the elements is 512^{-1} for $\Delta X_1(t)$, and 64^{-1} for $\Delta X_2(t)$.

VI. MULTI-SCALING ANALYSIS

The notion of multi-scaling, i.e., multi-affinity and multi-fractality, have been employed successfully in characterizing complex spatio-temporal behavior of various phenomena, such as velocity and energy dissipation fields in fluid turbulence [2,12], rough interfaces in fractal surface growth [13], nematic fluid electro-convective turbulence [14], financial data of currency exchange rates [15], and even in natural images [16]. In Ref. [6,11], we introduced multi-scaling analysis to our system for the one-dimensional case, inspired by the seeming similarity of the amplitude and difference fields in our system to the velocity and energy dissipation fields in fluid turbulence. Here, we attempt the multi-scaling analysis for the two-dimensional case.

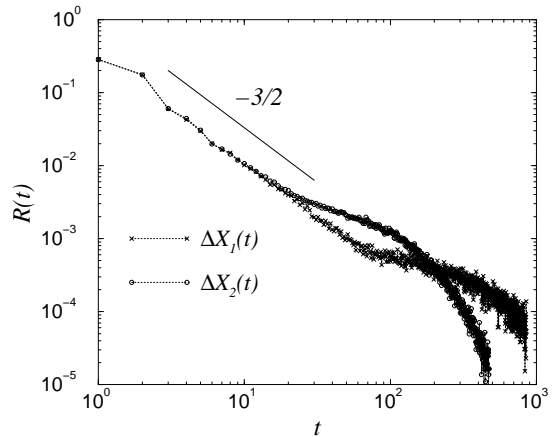


FIG. 7. Distributions of the laminar length obtained from the time sequences $\Delta X_1(t)$ and $\Delta X_2(t)$ shown in Fig.6.

First, we introduce the difference field $Z(\mathbf{r})$ as

$$Z(\mathbf{r}) := |\nabla X(\mathbf{r})| = \sqrt{\left(\frac{\partial X}{\partial x}\right)^2 + \left(\frac{\partial X}{\partial y}\right)^2}, \quad (14)$$

which emphasizes the edges of the original amplitude field $X(\mathbf{r})$ ². This quantity is an analogue of the energy dissipation field in fluid turbulence. Figure 8 shows a typical snapshot of the difference field $Z(x, y)$ at $K = 0.85$, corresponding to the amplitude field shown in Fig.2. The intermittency underlying the original amplitude field is now apparent.

We then introduce the following quantities as measures for the amplitude field $X(\mathbf{r})$ and the difference field $Z(\mathbf{r})$:

$$h(\mathbf{r}; l) := |X(\mathbf{r} + \mathbf{l}) - X(\mathbf{r})|, \quad (15)$$

$$m(\mathbf{r}; l) := \int_{S(\mathbf{r}; l)} Z(\mathbf{r}') d^2 \mathbf{r}', \quad (16)$$

where $|\mathbf{l}| = l$, and the domain of integration $S(\mathbf{r}; l)$ is a square of size l placed at \mathbf{r} . The first quantity is a difference of the amplitude field $X(\mathbf{r})$ between two points separated by a distance of l , and the second quantity is a volume enclosed by the difference field $Z(\mathbf{r})$ and the square $S(\mathbf{r}; l)$.

According to the multi-fractal formalism, two types of partition functions are defined as

$$Z_h^q(l) := \langle h(l)^q \rangle = \frac{1}{M(l)} \sum_{i=1}^{M(l)} h(\mathbf{r}_i; l)^q, \quad (17)$$

²Here, the differential should not be interpreted literally. We always use finite difference in the actual calculation, e.g. $(X(x + \Delta x, y) - X(x, y))/\Delta x$ with sufficiently small Δx , and this is important to observe the multi-scaling behavior [11].

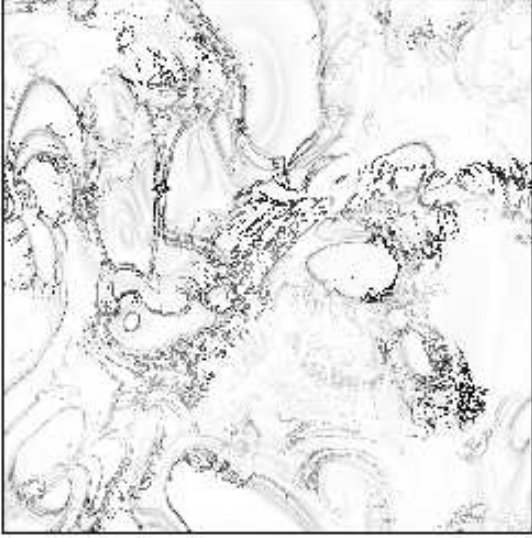


FIG. 8. Snapshot of the difference field $Z(x, y)$ at $K = 0.85$, corresponding to the amplitude field shown in Fig.2.

$$Z_m^q(l) := N(l) \langle m(l)^q \rangle = \sum_{i=1}^{N(l)} m(\mathbf{r}_i; l)^q, \quad (18)$$

where $Z_h^q(l)$ is calculated along a certain straight line in some direction as in the case of the previous spatial correlation function, while $Z_m^q(l)$ is calculated over the whole system. \mathbf{r}_i is either the position of the line segment or the position of the square. $M(l)$ is the number of line segments of length l that are needed to cover the entire line, and $N(l)$ is the number of squares of size l that are needed to cover the whole system. The function $Z_h^q(l)$ is called structure function in the context of fluid turbulence [2,12].

When the measures have scaling properties, the partition functions are expected to scale with l as $Z_h^q(l) \sim l^{\zeta(q)}$ and $Z_m^q(l) \sim l^{\tau(q)}$. Furthermore, if these exponents $\zeta(q)$ and $\tau(q)$ depend nonlinearly on q , the corresponding measures $h(l)$ and $m(l)$ are called multi-affine and multi-fractal, respectively [2,12,13].

For the one-dimensional case, we already know that the amplitude field is multi-affine and the difference field is multi-fractal. Moreover, our previous theory predicts the following form for the scaling exponent $\zeta(q)$ of the amplitude field:

$$\zeta(q) = q \quad (0 < q < \beta), \quad \beta \quad (\beta < q), \quad (19)$$

where β is a positive constant determined by the fluctuation of the finite-time Lyapunov exponent of the element, and is related to the slope of the probability distribution of $h(l)$ [6,11]. This is the simplest form of multi-affinity,

and sometimes called bi-fractality [12]³. The same form of the scaling exponent $\zeta(q)$ is also expected in two dimension, since our previous theory imposed no restriction on the dimensionality of the system.

For the scaling exponent $\tau(q)$ of the difference field, we have not been able to develop a satisfactory theory yet. Numerical results in one-dimensional systems suggest that $\tau(q)$ also depends nonlinearly on q , and the difference field is multi-fractal with a rather simple functional form for $\tau(q)$ [11]. However, the scaling exponent $\tau(q)$ for the two-dimensional system may be different from that for the one-dimensional case, since $Z_m^q(l)$ is defined depending on the dimensionality of the system, while $Z_h^q(l)$ is always defined along a one-dimensional line.

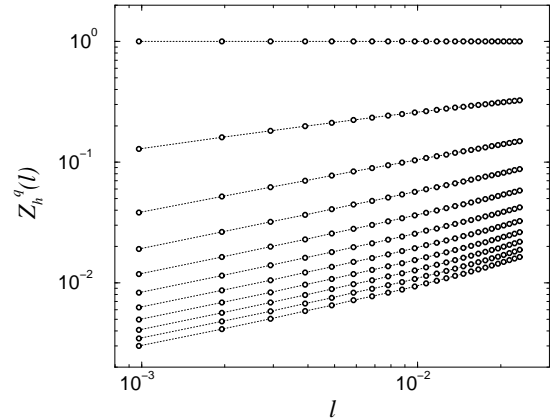


FIG. 9. Partition functions $Z_h^q(l)$ vs. l for several values of q . The top line corresponds to $q = 0$, and the bottom one to $q = 5$, at intervals of 0.5.

Let us proceed to the numerical results now. The coupling strength is fixed at $K = 0.85$ hereafter, where the system is fully in the anomalous spatio-temporal chaotic regime.

Figure 9 shows the partition function $Z_h^q(l)$ obtained for several values of q . Each curve depends on l in a power-law manner for small l , and its exponent increases with q . The dependence of the scaling exponent $\zeta(q)$ on q is shown in Fig.11. The $\zeta(q)$ curve is a strongly nonlinear function of q , and the multi-scaling property of the amplitude field is evident. Furthermore, the $\zeta(q)$ curve has a bi-linear form as expected in Eq.(19), although a sharp transition is absent due to the limited number of oscillators. From the large q behavior of the exponent, we can roughly estimate the value of β as ~ 0.48 .

Thus, the amplitude field turns out to be multi-affine,

³There is some confusion in terminology due to historical reasons. A word 'bi-affinity' will be more appropriate if it exists.

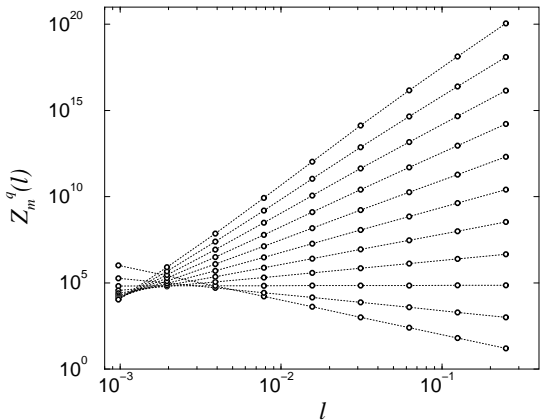


FIG. 10. Partition functions $Z_m^q(l)$ vs. l for several values of q . The bottom line corresponds to $q = 0$, and the top one to $q = 5$, at intervals of 0.5.

and the behavior of the scaling exponent is the same as that for the one-dimensional case.

Figure 10 shows the partition function $Z_m^q(l)$ for several values of q . It is clear that each curve shows a power-law dependence on l . The width of the region where the power law holds seems much wider than the previous case. The scaling exponent $\tau(q)$ is plotted with regard to q in Fig.12. The corresponding generalized dimension $D(q) := \tau(q)/(q - 1)$ is also shown in the inset. The $\tau(q)$ curve is again a nonlinear function of q , but its dependence on q does not seem to be so simple as that of the $\zeta(q)$ curve. However, as we conjectured numerically for the one-dimensional case [11], asymptotic linearity of the $\tau(q)$ curve seems to hold. Correspondingly, the $D(q)$ curve seems to saturate to a horizontal line $D(q) = D(\infty)$ quickly. But we can not observe a clear transition to the horizontal line as in the previous one-dimensional case, which may be due to the limited number of oscillators, or the two-dimensionality of the system.

Thus, the difference field also turns out to be multifractal. The behavior of the scaling exponent somewhat resembles that in the one-dimensional case, but is not completely the same.

VII. PROBABILITY DISTRIBUTIONS OF THE MEASURES

The multi-scaling properties of amplitude and difference fields are consequences of intermittency underlying the system. In order to analyze this intermittency in more detail, we study here the probability distribution functions (PDF) of both measures at each length scale.

Let us consider the PDFs of the measures $h(l)$ and $m(l)$. It is convenient to use rescaled measures $h_r(l) := h(l)/l$, $m_r(l) := m(l)/l^2$ and corresponding rescaled PDFs $P_r(h_r; l)$, $Q_r(m_r; l)$. With this rescaling, the peaks

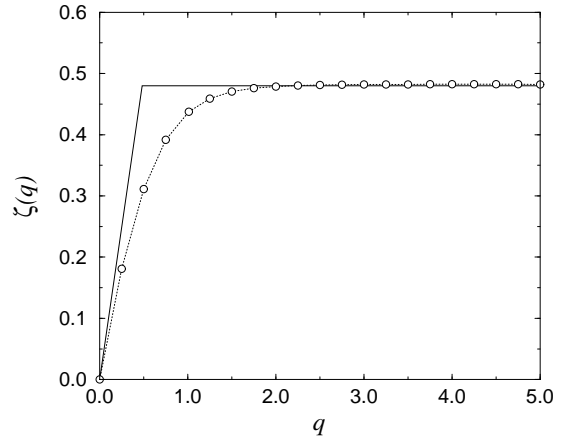


FIG. 11. Scaling exponent $\zeta(q)$ vs. q . The theoretical curve Eq.(19) with $\beta = 0.48$ is compared with the experimental data.

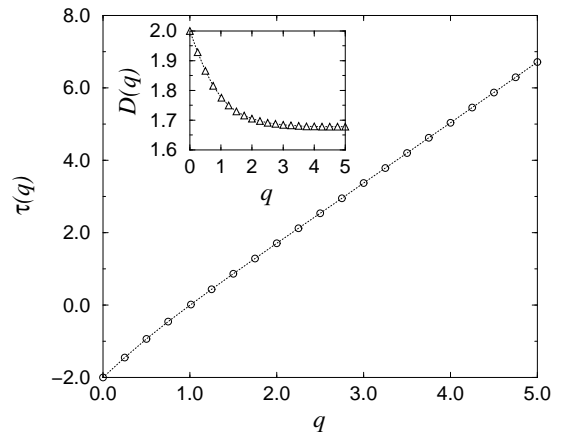


FIG. 12. Scaling exponent $\tau(q)$ vs. q . The inset shows the corresponding generalized dimension $D(q)$ vs. q .

and the widths of the PDFs become relatively close. We show our results in these rescaled variables.

The scaling exponents $\zeta(q)$ and $\tau(q)$ are fully determined by the dependence of these PDFs on the scale l . In Ref. [11], we approximated the tails of the PDFs by certain functional forms and extracted the scaling exponents asymptotically in the small l limit. Here we present the numerical results only briefly for the purpose of emphasizing the intermittency of the amplitude and difference fields.

Figure 13 shows the rescaled PDF $P_r(h_r; l)$ of the rescaled amplitude difference $h_r(l)$ for several values of l in log-log scales. Each PDF has a characteristic truncated Lévy-like shape, as we already obtained previously for the one-dimensional case; it is composed of a constant region near the origin, a power-law decay in the middle, and a sharp cutoff. Each curve roughly collapses to a scale-invariant curve in the constant and power-law regions, while the cut-off of the tail moves to the right with decreasing of l due to the intermittency. More precisely, the cut-off position of the PDF (defined in some suitable way) is proportional to l^{-1} . This gives rise to the bi-fractal behavior of the $\zeta(q)$ curve, see Ref. [11] for detail.

Our previous theory predicts that the slope of the power-law decay is given by $-1 - \beta$ with the constant β from Eq. (19). This is confirmed in Fig.13, where the slope of the power-law decay can be read off as -1.4 , roughly in agreement with the previously obtained value $\beta \sim 0.48$ from the scaling exponent $\zeta(q)$. The inset of Fig. 13 shows the PDF of the amplitude difference $h(l)$ (without taking the absolute value) rescaled by the standard deviation in linear-log scales, in order to further emphasize the intermittency of the amplitude field. The PDF evolves from nearly Gaussian into intermittent power-law with the decrease of scale l .

Figure 14 shows the PDFs $Q_r(m_r; l)$ of the rescaled volume $m_r(l)$. Their shapes are not so simple as those for $P_r(h_r; l)$. They are also qualitatively different from the PDF for the difference field in the previous one-dimensional case [11], which is responsible for the slightly different behavior of the scaling exponent $\tau(q)$ from the one-dimensional case. But we can still see that both tails extend, and the distribution widens with the decrease of scale l . Namely, as we decrease the observation scale l , largely deviated events appear more frequently. It is obvious that this intermittency effect gives rise to the nonlinearity of the scaling exponent $\tau(q)$, although the precise functional form is difficult to obtain. The inset shows the PDF of the measure $m(l)$ rescaled by the standard deviation in linear-log scales for several values of l . The PDF gradually gets steeper with the decrease of l due to the intermittency.

Thus, the PDFs of the measures reveal the intermittency in our system clearly. Especially, the PDF for the amplitude difference $h(l)$ has the same shape as that already obtained in the one-dimensional case.

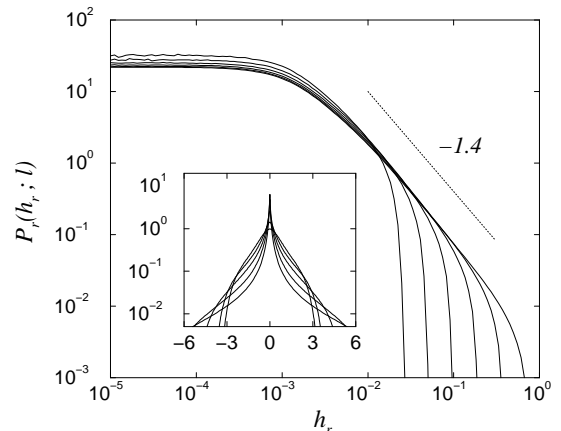


FIG. 13. Rescaled PDFs $P_r(h_r; l)$ for $l = \sqrt{2}, 2\sqrt{2}, 4\sqrt{2}, 8\sqrt{2}, 16\sqrt{2},$ and $32\sqrt{2}$ ($\times 10^{24}^{-1}$). The curve with the slowest cutoff corresponds to $l = \sqrt{2} \times 10^{24}^{-1}$, and the leftmost curve with the fastest cutoff corresponds to $l = 32\sqrt{2} \times 10^{24}^{-1}$. The inset shows PDFs of the amplitude difference $h(l)$ (without taking the absolute value) rescaled by the standard deviation in log-linear scales for $l = \sqrt{2}$ (the steepest curve), $4\sqrt{2}, 16\sqrt{2}, 64\sqrt{2}$, and $128\sqrt{2}$ (the nearly quadratic curve) ($\times 10^{24}^{-1}$).

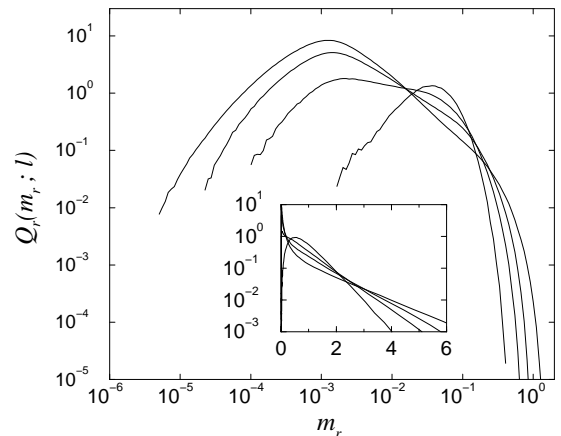


FIG. 14. Rescaled PDFs $Q_r(m_r; l)$ for $l = 2$ (the widest distribution with the steepest power-law decay), $8, 32, 128$ (the narrowest) ($\times 10^{24}^{-1}$). The inset shows PDFs of $m(l)$ rescaled by the standard deviation in log-linear scales for the same set of l values. The steepest curve corresponds to $l = 2 \times 10^{24}^{-1}$, and the curve with nearly quadratic peak corresponds to $l = 128 \times 10^{24}^{-1}$.

VIII. CONCLUSION

We numerically analyzed a two-dimensional system of non-locally coupled complex Ginzburg-Landau oscillators. As in the previous one-dimensional case, we found an anomalous spatio-temporally chaotic regime characterized by a power-law behavior of the spatial correlation function. As expected from our previous theory, the amplitude difference between neighboring elements exhibits noisy on-off intermittency, giving a microscopic dynamical origin for the power-law spatial correlations. We performed multi-scaling analysis in that regime, and found that the amplitude and difference fields are indeed multi-affine and multi-fractal, indicating strong intermittency underlying the system. By studying the PDFs of the measures at each length scale, the intermittency was clearly observed as scale-dependent deviations of the PDFs in their tails.

Multi-scaling properties are also known in various phenomena such as turbulence or fractal surface growth. The appearance of similar multi-scaling properties in many different systems implies some underlying common statistical law leading to such behavior. Further study of the intermittency in our system will give more insights and hints for the understanding of the multi-scaling properties observed in complex dissipative systems.

ACKNOWLEDGMENTS

The author gratefully acknowledges helpful advice and continuous support by Prof. Yoshiki Kuramoto, and thanks Dr. Axel Rossberg for a critical reading of the manuscript. He also thanks the Yukawa Institute for providing computer resources, and the JSPS Research Fellowships for Young Scientists for financial support.

-
- [1] Y. Kuramoto, *Chemical Oscillations, Waves, and Turbulence* (Springer-Verlag, Berlin, 1984).
 - [2] T. Bohr, M. H. Jensen, G. Paladin, and A. Vulpiani, *Dynamical Systems Approach to Turbulence* (Cambridge University Press, Cambridge, 1998).
 - [3] V. Hakim and W-J. Rappel, Phys. Rev. A **46** (1992), 7347 ; N. Nakagawa and Y. Kuramoto, Prog. Theor. Phys. **89** (1993), 313.
 - [4] K. Kaneko, Physica D **41** (1990), 137 ; T. Shibata and K. Kaneko, Phys. Rev. Lett. **81** (1998), 4116.
 - [5] Y. Kuramoto, Prog. Theor. Phys. **94** (1995), 321.
 - [6] Y. Kuramoto and H. Nakao, Phys. Rev. Lett. **76** (1996) 4352 ; Phys. Rev. Lett. **78** (1997) 4039.
 - [7] H. Nakao, Phys. Rev. E **58** (1998) 1591.
 - [8] A. S. Pikovsky, Phys. Lett. A **165** (1992), 33.

- [9] N. Platt, S. M. Hammel, and J. F. Heagy, Phys. Rev. Lett. **72** (1994), 3498.
- [10] A. Čenys and H. Lustfeld, J. Phys. A **29** (1996), 11 ; A. Čenys, A. N. Anagnostopoulos, and G. L. Bleris, Phys. Lett. A **224** (1997), 346.
- [11] H. Nakao and Y. Kuramoto, to be published in Eur. Phys. J. B.
- [12] U. Frisch, *Turbulence - The Legacy of A. N. Kolmogorov* (Cambridge University Press, Cambridge, 1995).
- [13] P. Meakin, *Fractals, scaling, and growth far from equilibrium* (Cambridge University Press, Cambridge, 1998).
- [14] V. Carbone, N. Scaramuzza, and C. Versace, Physica D **106** (1997), 314.
- [15] N. Vandewalle and M. Ausloos, Eur. Phys. J. B **4** (1998), 257.
- [16] A. Turiel, G. Mato, N. Parga, and J-P. Nadal, Phys. Rev. Lett. **80** (1998), 1098.